

Article

Arthropod Ectoparasites Have Potential to Bind SARS-CoV-2 via ACE

Su Datt Lam ^{1,2,*}, Paul Ashford ¹, Sandra Díaz-Sánchez ³, Margarita Villar ^{3,4}, Christian Gortázar ³, José de la Fuente ^{3,5,*} and Christine Orengo ^{1,*}

- ¹ Institute of Structural and Molecular Biology, UCL, Darwin Building, Gower Street, London WC1E 6BT, UK; p.ashford@ucl.ac.uk
- ² Department of Applied Physics, Faculty of Science and Technology, Universiti Kebangsaan Malaysia, Bangi 43600, Selangor, Malaysia
- ³ SaBio, Instituto de Investigación en Recursos Cinegéticos IREC-CSIC-UCLM-JCCM, Ronda de Toledo s/n, 13005 Ciudad Real, Spain; sandra.diaz@uclm.es (S.D.-S.); margaritam.villar@uclm.es (M.V.); Christian.Gortazar@uclm.es (C.G.)
- ⁴ Regional Centre for Biomedical Research (CRIB), Biochemistry Section, Faculty of Science and Chemical Technologies, University of Castilla-La Mancha, 13071 Ciudad Real, Spain
- ⁵ Center for Veterinary Health Sciences, Department of Veterinary Pathobiology, Oklahoma State University, Stillwater, OK 74078, USA
- * Correspondence: sudatt@ukm.edu.my (S.D.L.); josedejesus.fuente@uclm.es (J.d.l.F.); c.orengo@ucl.ac.uk (C.O.)

Abstract: Coronavirus-like organisms have been previously identified in Arthropod ectoparasites (such as ticks and unfed cat flea). Yet, the question regarding the possible role of these arthropods as SARS-CoV-2 passive/biological transmission vectors is still poorly explored. In this study, we performed *in silico* structural and binding energy calculations to assess the risks associated with possible ectoparasite transmission. We found sufficient similarity between ectoparasite ACE and human ACE2 protein sequences to build good quality 3D-models of the SARS-CoV-2 Spike:ACE complex to assess the impacts of ectoparasite mutations on complex stability. For several species (e.g., water flea, deer tick, body louse), our analyses showed no significant destabilisation of the SARS-CoV-2 Spike:ACE complex, suggesting these species would bind the viral Spike protein. Our structural analyses also provide structural rationale for interactions between the viral Spike and the ectoparasite ACE proteins. Although we do not have experimental evidence of infection in these ectoparasites, the predicted stability of the complex suggests this is possible, raising concerns of a possible role in passive transmission of the virus to their human hosts.

Keywords: SARS-CoV-2; COVID-19; spike protein; ACE2; structural bioinformatics; parasite



Citation: Lam, S.D.; Ashford, P.; Díaz-Sánchez, S.; Villar, M.; Gortázar, C.; de la Fuente, J.; Orengo, C. Arthropod Ectoparasites Have Potential to Bind SARS-CoV-2 via ACE. *Viruses* **2021**, *13*, 708. <https://doi.org/10.3390/v13040708>

Academic Editor:
Luis Martínez-Sobrido

Received: 2 April 2021
Accepted: 16 April 2021
Published: 19 April 2021

Publisher's Note: MDPI stays neutral with regard to jurisdictional claims in published maps and institutional affiliations.



Copyright: © 2021 by the authors. Licensee MDPI, Basel, Switzerland. This article is an open access article distributed under the terms and conditions of the Creative Commons Attribution (CC BY) license (<https://creativecommons.org/licenses/by/4.0/>).

1. Introduction

Arthropods such as mosquitoes, flies, lice, fleas, ticks and mites infest humans, wildlife and domestic animals and constitute a global health problem [1,2]. Ectoparasitic blood-feeding arthropods directly affect host health and also act as vectors of pathogenic bacteria, parasites and viruses [2]. Insect and arachnid ectoparasites represent a major burden for human and animal health worldwide and novel interventions are required for the control of ectoparasite infestations and transmission of pathogens [1,3,4]. Despite the development and possibilities of multiple control strategies, vaccines constitute the most effective and sustainable intervention for the control of ectoparasite infestations and vector-borne diseases [3,5,6].

Host–vector–pathogen molecular interactions evolved as conflict and cooperation [7]. In this way, arthropods may benefit from host factors and pathogen-induced gene expression that favour tick feeding and fitness, midgut microbiota composition and changes in epigenetic regulatory mechanisms that facilitate tick survival under extreme environmental

conditions, which results in evolutionarily conserved mechanisms that support pathogen infection with increased ectoparasite fitness and survival [7–12].

Arthropod ectoparasites may act as active biological transmission and/or passive transmission vectors of pathogenic microorganisms including viruses [13–18]. Viremia or infectious virus load detectable in vertebrate host circulating blood is required for biological transmission [13,18]. However, non-viremic arbovirus transmission is observed in viremia-free vertebrate hosts that play a role in disease epidemiology [13,18]. Biological vectors such as mosquitoes, mites, fleas, lice and ticks may carry pathogens that can multiply within their bodies for transmission to new hosts, usually by biting [14,19]. Mechanical vectors such as domestic flies, mosquitoes and ticks can collect infectious agents from contaminated objects, fluids and tissues and carry them on the outside (body exoskeleton, feet or mouth parts) or inside of their bodies and transmit them through physical contact with host body, food or drink [14]. In some vector–host–pathogen interactions, pathogens are transmitted both biologically after completing a life cycle in the vector and passively by intrastadial transmission (e.g., *Amblyomma hebraeum*–wild ungulates, domestic ruminants–lumpy skin disease virus, LSDV [20]) or from contaminated mouthparts to susceptible infested hosts (e.g., cat flea *Ctenocephalides felis*–cats, dogs, opossums, raccoons, rodents, humans–*Rickettsia felis* [21] and fly, *Stomoxys calcitrans*–cattle–*Anaplasma marginale* [22–24]). In other cases, only passive transmission through blood–meal regurgitation may occur (e.g., *Ornithodoros moubata*–human–HIV-1 [25]).

The hosts susceptible to severe acute respiratory syndrome coronavirus 2 (SARS-CoV-2) have a role in the coronavirus disease 19 pandemic (COVID-19) and are also infested by multiple blood-feeding arthropod ectoparasites [26–28]. Natural infections with SARS-CoV-2 have been reported in several animal species with evidence of zoonotic (animal-to-human) and reverse zoonotic (human-to-animal) virus transmission [28]. Coronavirus-like organisms have been previously identified in tick *Ixodes uriae* [29] and in unfed cat flea *Ctenocephalides felis* [30], thus raising the question of the possible role of ectoparasite arthropod vectors on SARS-CoV-2 passive and/or biological transmission [30].

Recently, models for SARS-CoV-2 Spike (S)-angiotensin I converting enzyme 2 (ACE2) host receptor interactions support that animal species with close-to-human S-ACE2 interactions (e.g., great apes or ruminants) may constitute effective hosts for maintenance and zoonotic transmission of the virus while other animal species with low S-ACE2 interaction capacity (e.g., cats or pigs) may be susceptible to reverse zoonotic transmission with low risk for human infection [31]. Additionally, the role of integrins also found in ectoparasite vectors [32] as co-receptors for SARS-CoV-2 and flavivirus cell attachment may also affect animal host susceptibility to infection [33,34]. Host- and virus-derived factors continue to be key drivers of the pandemic [35]. Based on the role of arthropod ectoparasites in pathogen passive and/or biological transmission and available preliminary evidence [29,30], the possible role of arthropod vectors in SARS-CoV-2 transmission needs to be considered.

We performed a number of protein structural and binding energy calculations to assess one of the steps in arthropod–pathogen interactions that may be associated with the risks of possible ectoparasite vector transmission. Since the complex formed between SARS-CoV-2 Spike protein and the human ACE2 receptor has been structurally determined (PDB code 6M0J [36]), we assessed whether the similarity of ectoparasite ACE proteins to human ACE2 was sufficient to model the SARS-CoV-2 Spike:ACE complex and assess the impacts of any residue mutations in ectoparasite ACE on the stability of this complex. We also performed detailed structural analyses to explore and characterise the possible structural mechanisms affecting complex stability. Our data suggest that there is sufficient similarity between ectoparasite ACE and human ACE2 protein sequences to build good quality 3D-models of the SARS-CoV-2 Spike:ACE complex to assess the impacts of ectoparasite mutations on complex stability. For several species where there were genomic data available (e.g., water flea, deer tick, body louse), our analyses showed no significant destabilisation of the SARS-CoV-2 Spike:ACE complex, suggesting these species would bind the viral Spike protein.

In support of the stability calculations, we provide structural rationale for interactions between the viral Spike and the ectoparasite ACE proteins.

Our analyses of complex stability employed a platform previously established to analyse possible SARS-CoV-2 infection in a wide range of animal species. This earlier work allowed us to establish thresholds on whether changes in stability of the SARS-CoV-2 Spike:ACE2 complex, caused by residue mutations in the animal, were likely to affect infection. We have applied the same computational platform and thresholds to assess changes in stability of the SARS-CoV-2 Spike:ACE complex in ectoparasites, some of which are blood-feeding arthropod ectoparasites. Although we do not have experimental evidence of infection in these ectoparasites, the predicted stability of the complex suggests this is possible, raising concern of a possible role in passive transmission of the virus to their human hosts.

2. Materials and Methods

2.1. Sequence Data

We obtained ACE protein sequences in fruit fly (*Drosophila melanogaster*; Uniprot ID: Q10714), water flea (*Daphnia pulex*; E9GU43), water flea order (*D. pulex*; A0A162PAD4), body louse (*Pediculus humanus corporis*; E0VAB8), deer tick (*Ixodes scapularis*; A0A4D5RPS5), and common tick (*Ixodes ricinus*; A0A0K8R3C7). We used NCBI BLAST v.2.6 [37,38] to align protein sequences to the human ACE2 sequence (Q9BYF1).

2.2. Structural Data

We used the structure of the SARS-CoV-2 spike protein (at 2.45 Å resolution (PDB ID 6M0J [36])) reference strain, bound to human ACE2 as a template to model the structures of the ectoparasite ACE bound to the SARS-CoV-2 reference (Wuhan-Hu-1) and the ectoparasite ACE protein bound to different strains of the SARS-CoV-2 with mutations at various sites in the RBD.

Models were built by generating query–template alignments using HH-suite version 3 [39], which were then used as input to the MODELLER v.9.24 program [40,41]. To optimise the geometry of the complex and interface we used the ‘very_slow’ schedule for model refinement. Ten models were generated for each S-protein:ACE complex and we then selected the model with the lowest normalised DOPE score (nDOPE) [42], which reflects the quality of the model. Positive scores are likely to be poor models, while scores lower than −1 are likely to be native-like.

2.3. Identification of Residues Involved in Binding of Viral SARS-CoV-2 to Host ACE

In order to determine the impact of mutations occurring between the ectoparasite ACE sequences and human sequences, on the stability of the SARS-CoV-2 S:ACE complex, we identified key residues in the interface of these proteins. In addition to residues in ACE2 that contact the S-protein directly, we also included residues that are in the second shell, or are buried, and could influence binding, as previous studies showed that mutations in these positions correlated well with experimental data on changes in complex stability [43]. Therefore, we used the following sets of residues for our study:

Direct contact (DC) residues: These are in direct contact with the S-protein [36] identified by PDBe [44] and PDBSum [45]. We identified 20 residues.

Direct contact extended (DCEX) residues: We identified residues within 8 Å of DC residues which are likely to be important for binding. We used detailed manual inspection of the complex, and also selected residues according to (i) evidence from deep mutagenesis studies [41], (ii) in silico alanine scanning analyses (using mCSM-PPI2 [46]), (iii) high evolutionary conservation of the residues identified by the FunFam-based protocol described above, i.e., residues identified with DOPS [47] ≥ 70 and ScoreCons [47] score ≥ 0.7 , (iv) allosteric site prediction [48–50], and (v) sites under positive selection [51–53]. We also included residues identified by other related structural analyses, reported in the literature [36,43,54–57].

2.4. Measuring Change in Residue Chemistry for Mutations

For each ectoparasite, we computed the Grantham score [58] comparing the ectoparasite ACE to the human ACE2 in order to understand the chemical shift associated with mutations involving the interface binding residues. Grantham score calculates volume, polarity, and atomic composition differences between amino acids. A Grantham score ranges from 0 to 215; higher Grantham scores are considered more disruptive to interface stability. The sums of Grantham scores were obtained for both DC and DCEX residues.

2.5. Measuring Changes in the Stability of the S-Protein:ACE Complex. Following Mutation

We calculated the change in stability of the S-protein:ACE complex using mCSM-PPI2 [46]. This method was used in a previous analysis to analyse the impacts of mutations on the stability of the S-protein:ACE2 complex and was verified using data from in vitro and in vivo studies [31]. mCSM-PPI2 exploits machine learning models that analyse graph-based signature vectors for each mutation to predict the binding energy. The signature vector encodes multiple features including atom-distance patterns in the wild-type protein, pharmacophore information, available experimental information, evolutionary information and energetic terms. The mCSM-PPI2 server (http://biosig.unimelb.edu.au/mcsm_ppi2/, accessed on 1 January 2021) was used for the simulations.

We produced ectoparasite ACE: SARS-CoV-2 Wuhan-Hu-1 complexes, ectoparasite ACE: SARS-CoV-2 N501Y complexes, and ectoparasite ACE: SARS-CoV-2 K417N, E484K, N501Y complexes. Using the model of ectoparasite ACE: SARS-CoV-2 complex, we mutated the ectoparasite ACE interface residues back to the appropriate residues found in the human ACE2 structure using mCSM-PPI2 to obtain the $\Delta\Delta G$ value. Positive $\Delta\Delta G$ values reflect destabilisation of the complex by the mutation and negative values reflect stabilisation of the complex.

2.6. Structural Analysis

We also evaluated structural changes for all combinations of RBD mutations and receptor complexes. We performed manual inspection of these key regions and others identified from studies by other groups [36,43,54–57,59]. We used UCSF Chimera v1.15 [60,61] to render structural images and predict H-bonds and salt bridges. Since all the 3D models were built using the very slow refinement option in MODELLER v9.24 [40,41], side-chain rotamers had been optimised. However, we also relaxed the allowable H-bond angle constraint to identify possible H-bonds at key hotspot residues.

2.7. Phylogenetic Analyses of Cytochrome Oxidase Subunit 1

We performed a phylogenetic analysis using nine cytochrome oxidase subunit 1 (COI) nucleotide sequences downloaded from GenBank to generate a robust phylogenetic tree (GenBank Accession Numbers: JX150976; KY322738; MG432684; KX360345; MK140087; LC029557; MK905394; KX054334; outgroup: JF871600). The nucleotide sequences were aligned with MAFFT [62] using Geneious Prime v2.2 software [63] (<https://www.geneious.com>, accessed on 1 January 2021). Further, jModelTest2 was computed using the AIC (Akaike Information Criteria) to select the best nucleotide substitution model [64]. Genetic distance was computed using General Time Reversible model and gamma distributed rate variation among sites (GTR + G) [65]. The phylogenetic tree was inferred according to the Maximum Likelihood method with 100 bootstrap replicates using Maximum Likelihood in MEGAX software [66,67]. Phylogenetic tree annotation and visualization was performed using FigTree v1.4.4 (<http://tree.bio.ed.ac.uk/>, accessed on 1 January 2021).

2.8. Methods for Pan-Taxonomic Metazoan Comparison Analysis

To analyse sequence relationships across the tree of life, we include 24 pantaxonomic compara species found in the Ensembl Metazoa database [68]. However, we found ACE sequences for only 17 species. We compared these ACE sequences with human ACE2 sequences using NCBI BLAST v.2.6 [37,38]. We also used EMBOSS Needle [69] to calculate

their sequence similarity with human ACE2 DCEX residue. A phylogenetic tree of invertebrate metazoan ACE DCEX residues was inferred using the Neighbour Joining method and BLOSUM62 substitution matrix.

3. Results

3.1. Comparison of Ectoparasite ACE with Human ACE2 Sequences

We compared the ectoparasite ACE with human ACE2 sequences using BLAST and found relatively high levels of sequence similarity (>35% in all cases), sufficient enough to model the structures for these proteins on the human ACE2 structure (Table 1).

Table 1. BLAST sequence identities of ectoparasite ACEs and human ACE2.

| Organism | Sequence Identity | E-Value |
|------------------------------|-------------------|-------------------------|
| A0A162PAD4, water flea order | 40.1% | 1.99×10^{-155} |
| A0A4D5RPS5, deer tick | 38.9% | 1.30×10^{-149} |
| A0A0K8R3C7, common tick | 37.7% | 5.29×10^{-136} |
| E0VAB8, body louse | 39.6% | 3.63×10^{-145} |
| E9GU43, water flea | 39.6% | 6.60×10^{-159} |
| Q10714, fruit fly | 36.3% | 1.31×10^{-139} |

3.2. How Many Mutated DCEX Residues Are There in the Interface and How Strong Are the Chemical Shifts?

We calculated the number of mutated DCEX residues (direct contact residues and residues within 8 Å of direct contact residues likely to influence binding, see Materials and Methods) and the Sum Grantham score (chemical shift) for mutation of these residues between ectoparasite and human sequences (Table 2).

Table 2. Mutated direct contact (DC), DCEX residues and the Sum Grantham score of ectoparasite ACEs.

| Organism | Number of Mutated DC Residues | Number of Mutated DCEX Residues | Sum Grantham Score |
|------------------|-------------------------------|---------------------------------|--------------------|
| Water flea order | 16 | 34 | 2795 |
| Deer tick | 16 | 34 | 2581 |
| Common tick | 17 | 34 | 2790 |
| Body louse | 14 | 33 | 2561 |
| Water flea | 15 | 34 | 2895 |
| Fruit fly | 15 | 35 | 2580 |

The number of mutations and differences in the chemical properties of the mutated residues, compared to the human residue, are quite large. However, our previous analyses contrasting a wide range of animal ACE2 proteins with human ACE2 demonstrated that changes of this order did not necessarily disrupt binding of CoV2: Spike with host ACE2 protein [31].

3.3. Modelling the Structure of the SARS-CoV-2 Spike:ACE Complex. for the Ectoparasites (Based on the Wuhan-Hu-1 Strain) and Calculating the Change in Stability of the Complex. Compared to Human

In order to explore whether the changes between the ectoparasite ACEs and the human ACE2 would be likely to destabilise the Spike: ACE2 complex, we modelled the 3D structure of the Wuhan-Hu-1 S-protein: ectoparasite ACE complex using our FunMod modelling platform [70,71]. We used PDB 6M0J as the template. The quality of the models is given by the normalised DOPE scores shown in Table 3 below. It can be seen that the models all have nDOPE scores less than -1 , indicating good quality models [40].

Table 3. Normalised DOPE scores of SARS-CoV-2 Wuhan-Hu-1 S-protein: ectoparasite ACE complexes.

| Organism | nDOPE Score |
|------------------|-------------|
| Water flea order | −1.12 |
| Deer tick | −1.26 |
| Common tick | −1.09 |
| Body louse | −1.03 |
| Water flea | −1.11 |
| Fruit fly | −1.10 |

For each complex, the change in stability of the complex, $\Delta\Delta G$, was predicted by mutating the ectoparasite ACE interface residue to the appropriate residue in the human ACE2. In our previous analysis, any animals with predicted $\Delta\Delta G \leq 3.72$ were considered to be at risk as these values correlated well with experimental evidence for infection [31]. Table 4 shows the $\Delta\Delta G$ values when considering direct contact (DC) residues and also for direct contact plus extended residues (DCEX, i.e., residues within 8Å of the DC residues). Red values highlight those indicating low destabilisation and therefore risk of infection.

Table 4. Predicted $\Delta\Delta G$ values of SARS-CoV-2 Wuhan-Hu-1 S-protein: ectoparasite ACE complexes for direct contact (DC) residues and also for direct contact plus extended (DCEX) residues. Ectoparasites are categorised according to risk of infection by SARS-CoV-2, with $\Delta\Delta G \leq 3.72$ being at risk (red), and $\Delta\Delta G > 3.72$ not at risk (blue).

| Organism | Predicted $\Delta\Delta G$ (DC) | Predicted $\Delta\Delta G$ (DCEX) |
|------------------|---------------------------------|-----------------------------------|
| Water flea order | 5.99 | 7.43 |
| Deer tick | 1.60 | 2.77 |
| Common tick | 1.97 | 2.79 |
| Body louse | −2.31 | −1.17 |
| Water flea | −1.33 | −0.53 |
| Fruit fly | 5.88 | 4.16 |

3.4. Structural Analyses of the Changes in the Interface of the SARS-CoV2 Spike: ACE Complex. (Wuhan-Hu-1 Strain) Relative to the Human Complex

We used the LIGPLOT program of PDBsum [72] to examine possible residue interactions between the Spike S protein and the ACE proteins, contrasting interactions in human proteins with those for the ectoparasite proteins. Several studies have highlighted the importance of key interaction sites between RBD of Spike S protein and ACE2, in particular, three sites on the interface: hydrophobic pocket, hotspot-353 and hotspot-31 [73]. These sites have previously been identified [74] as key to understanding why the SARS-CoV-2 S-protein binds to human ACE2 with high affinity and how the viral S-protein has evolved to bind with much higher affinity to human ACE2 than SARS-CoV [36,63,75].

It can be seen from Figure 1 below that a number of hydrogen bonds have been lost in the ectoparasites, including some for these key interaction sites. However, for some of the ectoparasites (i.e., water flea, body louse and deer tick) there has been an increase in non-bonded contacts, and these are distributed across the whole interface.

UCSF Chimera was also used to visually inspect these changes on the 3D structures of the complexes. Whilst human S-protein:ACE2 interface has close contacts across the whole interface including nine predicted H-bonds, the ectoparasites have very few hydrogen bonds (Figure 2). There are other structural changes that could also contribute to differences in the overall stability. However, as mentioned above these may be compensated for by the increase in non-bonded contacts. Deer tick and water flea have ~60 non-bonded contacts compared to ~80 in human, whilst body louse has ~130 across the whole interface, which may explain the small increase in stability of the S-protein:ACE complex relative to human. These ranges of $\Delta\Delta G$ value are probably within the error range for this method. Nevertheless, there is some structural rationale to support the suggestion that the complexes formed for these ectoparasites could be stable enough to support binding.

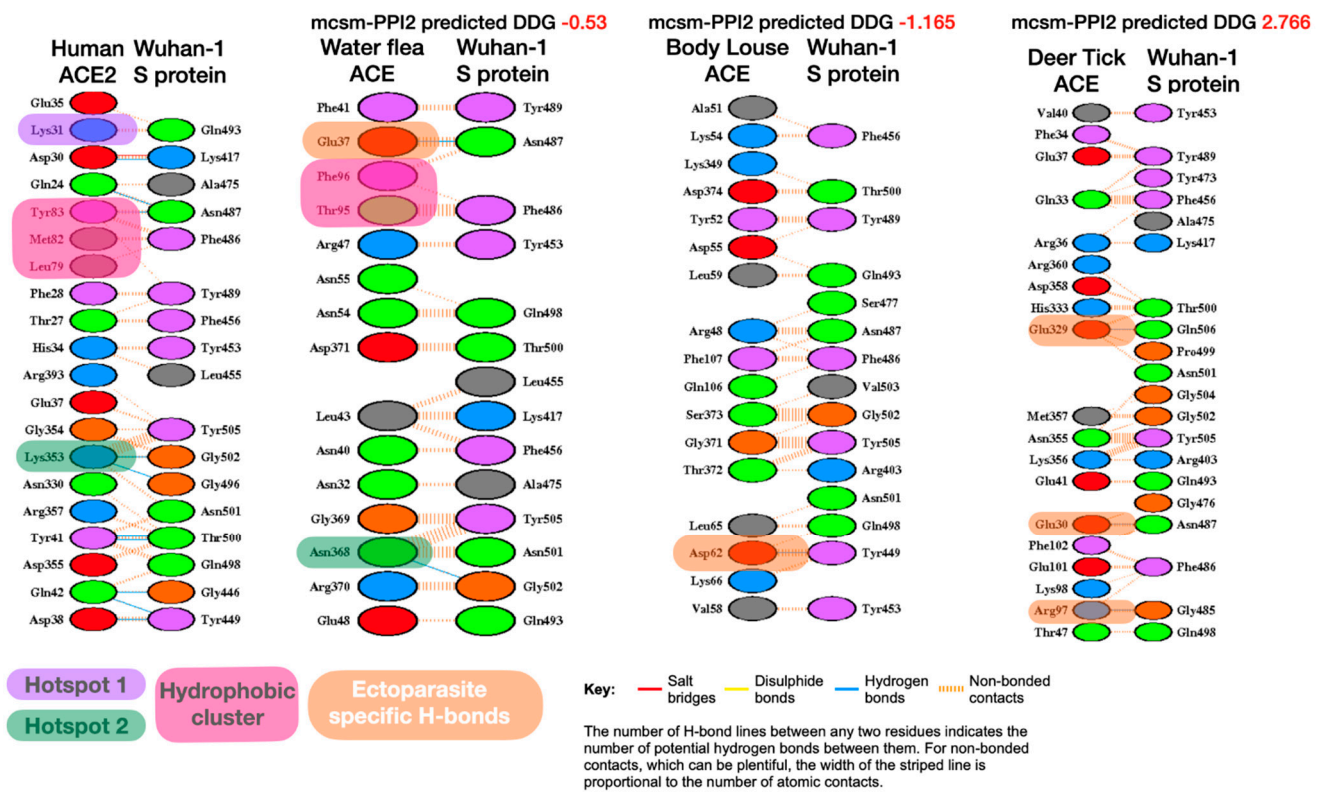


Figure 1. Comparison of LigPlot predicted bonding interactions for Wuhan-Hu-1 strain with human, water flea, body louse and deer tick. Corresponding residues in each species with key human interface hotspots (Hotspot 1, Hotspot 2) and the hydrophobic pocket are indicated if they are predicted to be involved in interface interactions. Novel ectoparasite H-bond residues also shown (pale orange boxes).

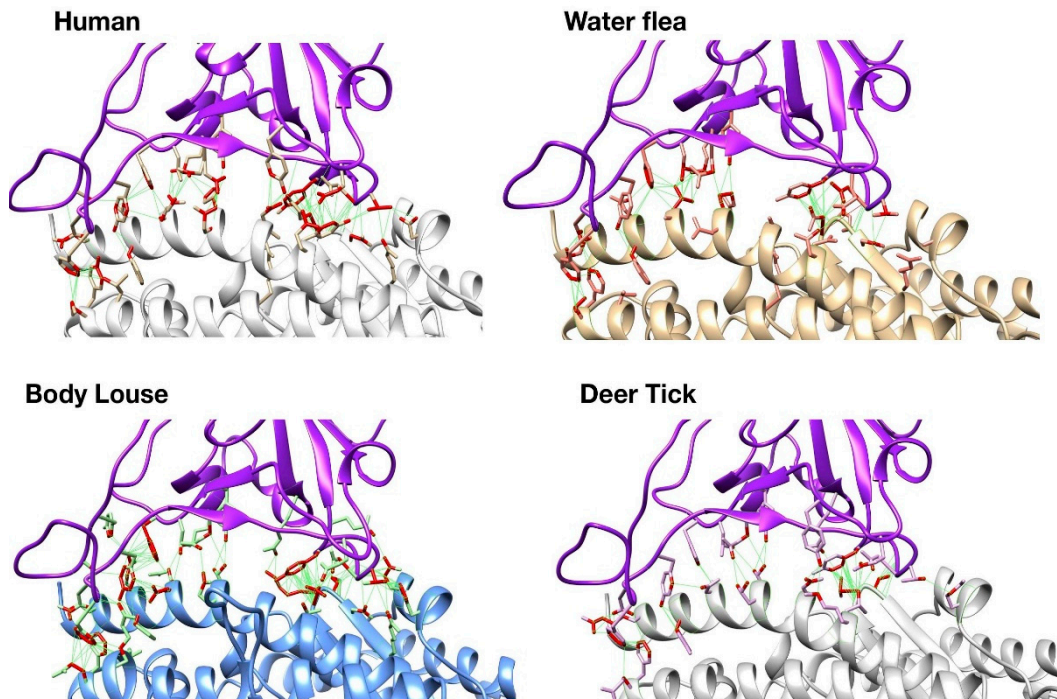


Figure 2. Structures of human and modelled ectoparasite SARS-CoV-2 S-protein: ACE complexes.

3.5. N501Y Mutant

In order to explore the likely impacts of the recent N501Y variant strain of SARS-CoV-2, we also modelled the N501Y S-protein: ectoparasite ACE using our modelling platform. We used 6M0J as the template. Again, good quality models were obtained for all the ectoparasite S-protein:ACE complexes (Table 5).

Table 5. Normalised DOPE scores of SARS-CoV-2 N501Y S-protein: ectoparasite ACE complexes.

| Organism | nDOPE Score |
|------------------|-------------|
| Water flea order | −1.15 |
| Deer tick | −1.23 |
| Common tick | −1.15 |
| Body louse | −0.93 |
| Water flea | −1.18 |
| Fruit fly | −1.09 |

For each complex, $\Delta\Delta G$ values were predicted by mutating the ectoparasite ACE interface residue to the appropriate residue in the human ACE2 (Table 6). As in our previous analysis, any animals with predicted $\Delta\Delta G \leq 3.72$ are considered to be at risk. Interestingly, we observe that this mutation in the spike RBD domain results in a slightly increased stability of the complex for body louse, calculated over the DCEX residues ($\Delta\Delta G$ -1.92 N501Y versus-1.17 Wuhan-Hu-1).

Table 6. Predicted $\Delta\Delta G$ values of SARS-CoV-2 N501Y S-protein: ectoparasite ACE complexes for direct contact (DC) residues and also for direct contact plus extended (DCEX) residues. Ectoparasites are categorised according to risk of infection by SARS-CoV-2, with $\Delta\Delta G \leq 3.72$ being at risk (red), and $\Delta\Delta G > 3.72$ not at risk (blue).

| Organism | Predicted $\Delta\Delta G$ (DC) | Predicted $\Delta\Delta G$ (DCEX) |
|------------------|---------------------------------|-----------------------------------|
| Water flea order | 5.49 | 7.18 |
| Deer tick | 1.72 | 1.67 |
| Common tick | 1.25 | 0.24 |
| Body louse | −2.17 | −1.92 |
| Water flea | −2.37 | −1.81 |
| Fruit fly | 7.13 | 5.99 |

Again, LIGPLOT analysis and visual inspection of the structures was performed to explore the rationale for the stability results (Figure 3).

Figure 4 shows that the N501Y mutation is predicted to more readily form H-bonds in part of the Spike:ACE interface in body louse (yellow circle) due to favourable geometry and the proximity of Tyrosine hydroxyl group to ACE interface residues. This H-bond (Tyr501-Thr47) enabled by the N501Y mutation stabilises part of the interface in body louse by binding to the ACE2 residue Thr47. It is within 5Å of the ‘Lys-353 hotspot’ identified as an important component of the Spike:human-ACE2 interface [73]. In body louse, Lys353 is replaced by Asn355; it is therefore possible that Tyr501-Thr47 provides an alternative H-bond component to the interface stability near this ‘hotspot353’ region.

Whilst there is a slight reduction in the number of non-bonded contacts relative to the Wuhan-Hu-1 strain, the N501Y Body Louse still has >100 non-bonded contacts across the interface combined with H-bond stabilisation at two distinct patches.

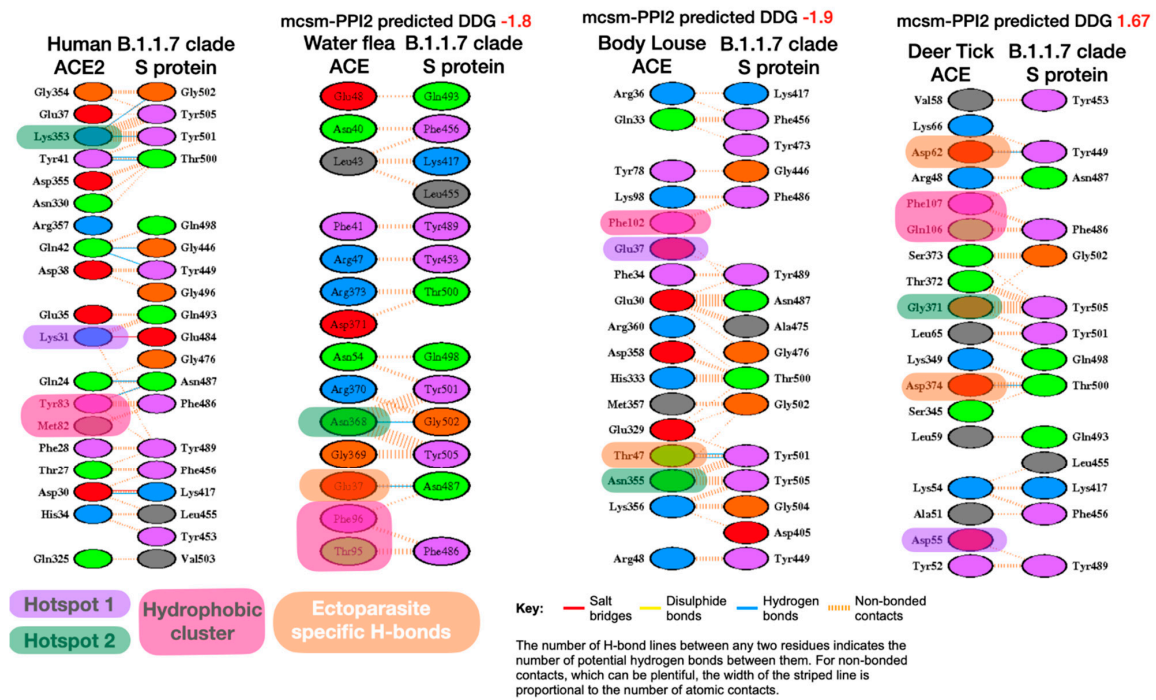


Figure 3. Comparison of LigPlot predicted bonding interactions for B.1.1.7 clade with human, water flea, body louse and deer tick. Corresponding residues in each species with key human interface hotspots (Hotspot 1, Hotspot 2) and the hydrophobic pocket are indicated if they are predicted to be involved in interface interactions. Novel ectoparasite H-bond residues also shown (orange boxes). In body louse, the ectoparasite-specific H-bond between Thr47 and Tyr501 is indicated as an equivalent to the important ‘Hotspot 2’ found in human spike:ACE2 interface.

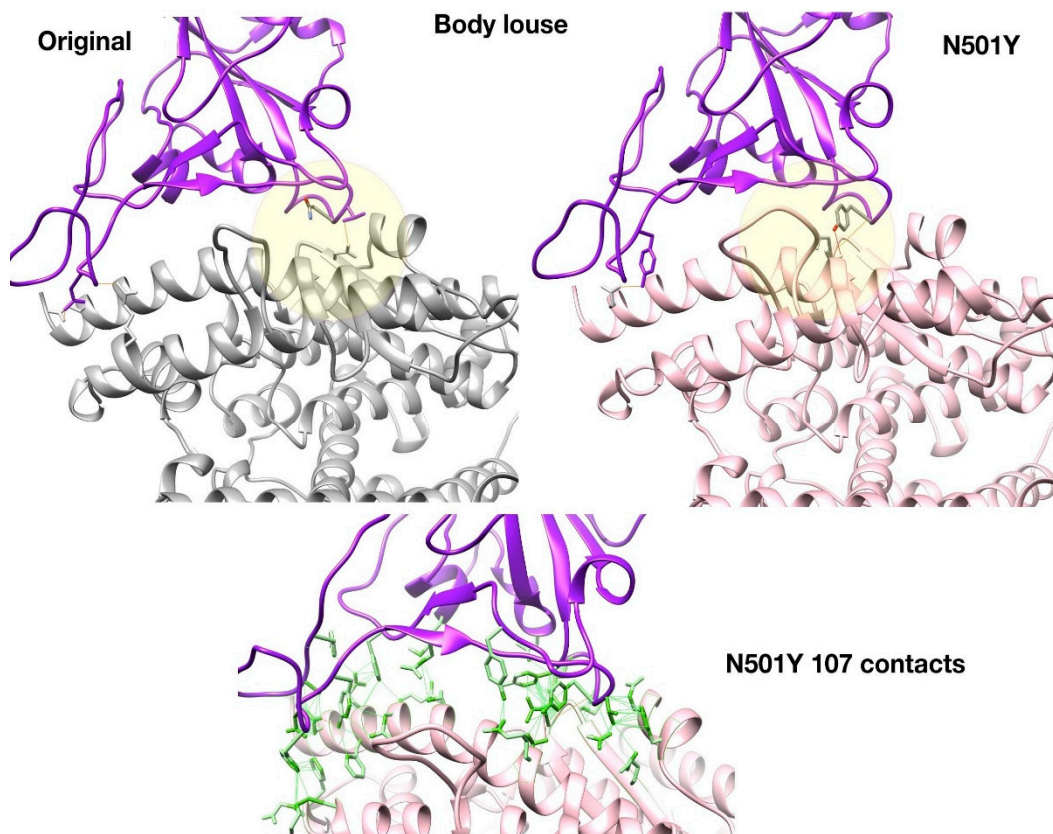


Figure 4. Structures of N501Y mutant show increased H-bond stabilisation in body louse.

3.6. K417N, E484K, N501Y Mutants

We also explored the impact of the combined variants observed in recent strains from South Africa and Brazil by modelling K417N, E484K, N501Y S-protein: ectoparasite ACE using our modelling platform (Figures S1 and S2, Tables S1 and S2). As with the N501Y mutant, we found that the combined variants had the effect of further stabilising the complex for body louse, water flea and the common tick. Structural analyses indicate that H-bonding in this strain could be behind the relatively high interface stability predicted for water flea and body louse according to the $\Delta\Delta G$ values. Limited H-bonds were predicted for deer tick, in agreement with the overall weaker predicted $\Delta\Delta G$ for this interface.

3.7. Phylogenetic Analysis

As mentioned above, coronavirus-like organisms have been previously identified in sea bird tick *Ixodes uriae* [29] and in unfed cat flea *Ctenocephalides felis* [30]. We were unable to obtain both sea bird tick and cat flea ACE sequences. Therefore, to understand the relationship between these ectoparasites we produced a phylogenetic tree using cytochrome oxidase subunit 1 (COI) sequences. Figure 5 below demonstrates that cat flea COI belongs to the same clade as body louse COI. Sea bird tick COI belongs to the same clade as deer tick and common tick COIs. Other ectoparasite species in the tree could not be analysed using our protocol since their ACE sequences were also unavailable.

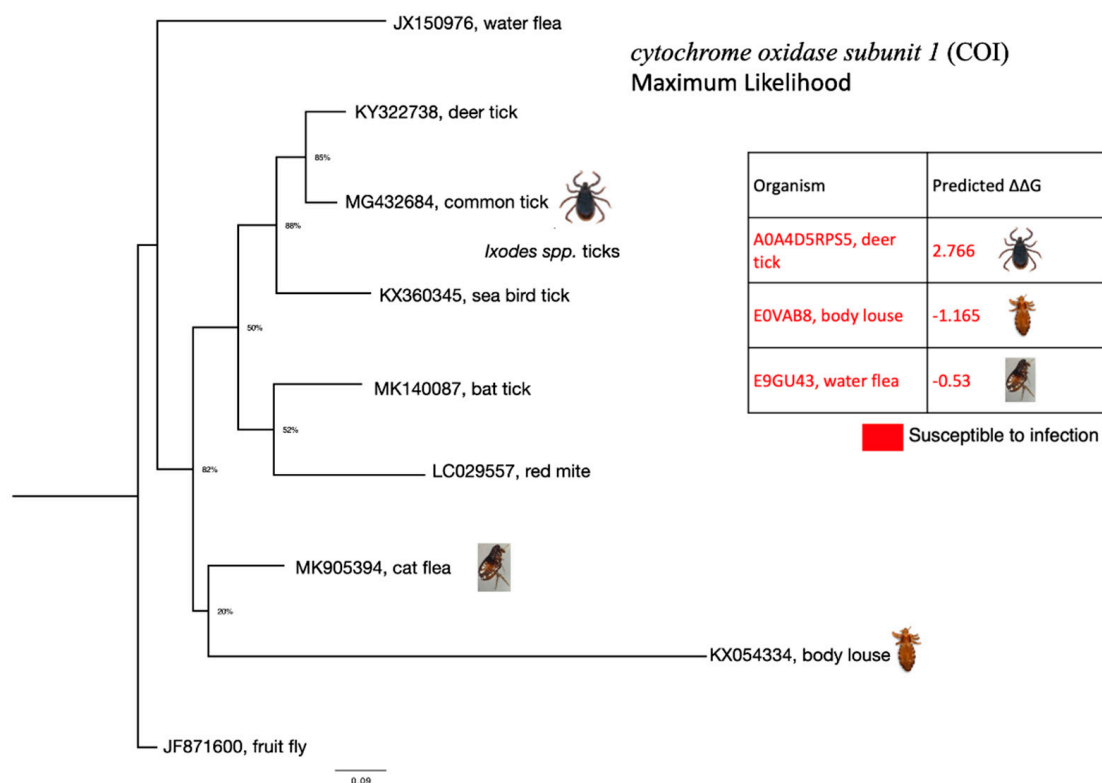


Figure 5. Phylogenetic tree of ectoparasite cytochrome oxidase subunit 1 (COI) nucleotide sequences. The phylogenetic tree was inferred according to the Maximum Likelihood method. Genetic distance was computed using General Time Reversible model and gamma distributed rate variation among sites (GTR + G).

3.8. Pan-Taxonomic Metazoan Comparison

We examined whether the significant similarity of ectoparasite ACE to human ACE2 (~40% sequence identity or higher) and the stable complex formed with SARS-CoV-2 Spike protein suggested selection pressure on the virus to evolve binding affinity to both animal hosts and their insect hosts. To do this, we performed a pantaxonomic analysis to determine the $\Delta\Delta G$ values for a range of invertebrate species (Figures S3–S7, Tables S3–S6). It can be

seen from Figure S6 that other invertebrates also have low $\Delta\Delta G$ values, including several species (octopus, African spider, honeybee) that are not ectoparasites, suggesting that the stability of the SARS-CoV-2 S-protein:ACE complex is not a result of selection pressure on the virus to evolve binding affinity to both animal hosts and their insect hosts.

4. Discussion

We have been able to obtain the protein sequences of ACE proteins and model the structural complexes of CoV2 Spike S-protein:ACE proteins in five ectoparasite species. The levels of sequence similarity between the ectoparasite sequences and the human ACE2 sequence suggested the possibility of similarity in the protein interface. Our energetic analyses, which examined the likely impacts of mutations between the human/ectoparasite sequences, showed a slight destabilisation in the complex for deer tick and common tick, whilst for the water flea and the body flea slight increases in stability of the complex were observed ($\Delta\Delta G < 0$). All the $\Delta\Delta G$ values measured were small and within the range of values observed in a previous study of animal hosts [31] as being likely to be associated with susceptibility to infection. As mentioned above, we are not suggesting infection of the parasites as there are currently no experimental data to support that but our data suggest that the virus would be able to attach to membrane-associated proteins (e.g., ACE) on the ectoparasite cell surface and that this may provide a mechanism for passive transmission of the virus.

Based on the results of this study and previous evidence on the role of arthropod vectors in biological and passive virus transmission [76] and the presence of coronaviruses in ticks and cat flea [29,30], our hypothesis is that insects and arachnids could have a potential role in SARS-CoV-2 transmission. Current evidence does not support SARS-CoV-2 vector biological transmission. However, the prolonged environmental stability of the virus [77,78] and putative interactions with vector ACE2 and integrin proteins suggest a possibility for SARS-CoV-2 passive transmission. Virus passive transmission may occur via contact with SARS-CoV-2-contaminated substrates and surfaces and/or through contaminated mouthparts, blood-meal regurgitation or mechanisms similar to RNA interference (RNAi) [79].

Infestations with blood-sucking arthropod ectoparasite vectors have been documented in animal species reported or predicted to host SARS-CoV-2 as in humans (Figure 6) [80–83]. Furthermore, ACE and integrin alpha and beta proteins have been identified in cat flea exoproteome [30,84] and tick salivary glands and cement [85], thus supporting membrane exposure and secretion of these molecules. As documented in ticks and in other arthropods [79,86], RNAi is based on the entry of exogenous or viral double-stranded RNA (dsRNA) into the cytoplasm through injection, feeding or virus production of dsRNA resulting in transstadial and inherited (transovarial) RNAi. Accordingly, it is possible that SARS-CoV-2 may be acquired by feeding ectoparasites and through interactions with ACE and integrins it may persist not only in contaminated mouthparts, but also inside the vector for transmission to susceptible hosts by blood-meal regurgitation during secondary feeding or after transstadial transmission or inherited virus RNA. In support of the possibility of inherited virus, coronavirus-derived proteins and RNA were identified in adult unfed cat flea [30].

Using the flea as a model arthropod vector [87], SARS-CoV-2 passive transmission may occur via different routes (Figure 7). If proven true in experimental animal trials, these results add a new player to the SARS-CoV-2 persistence and transmission and possible selection of new virus variants.

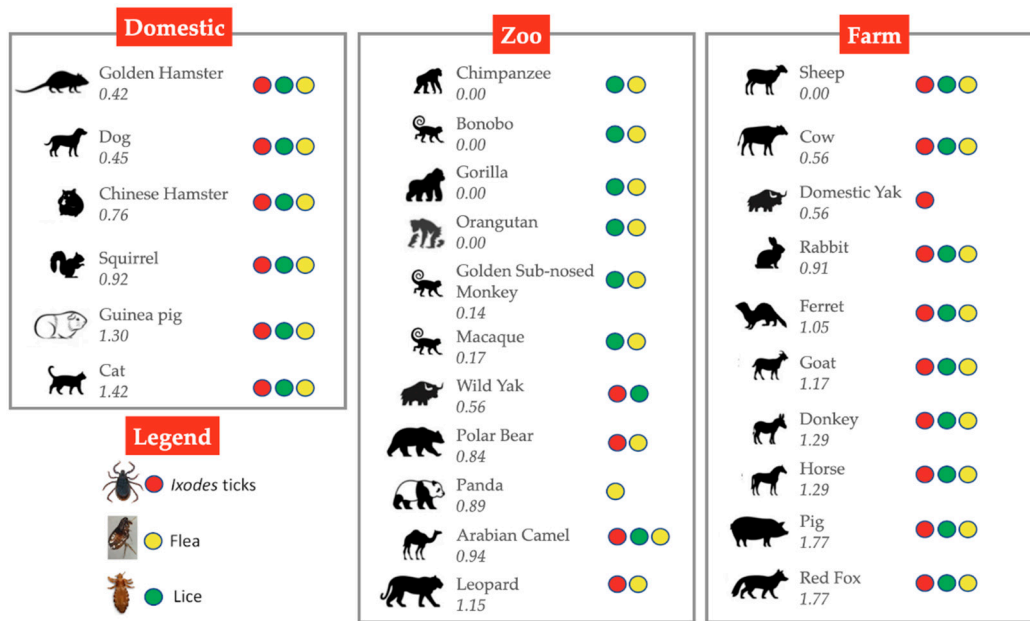


Figure 6. Animal hosts for ectoparasites. These animal hosts may be in contact with humans in domestic, agricultural or zoological settings. Numbers represent the predicted change in binding energy ($\Delta\Delta G$) of the S-protein:ACE2 [31]. Supporting references [80–83].

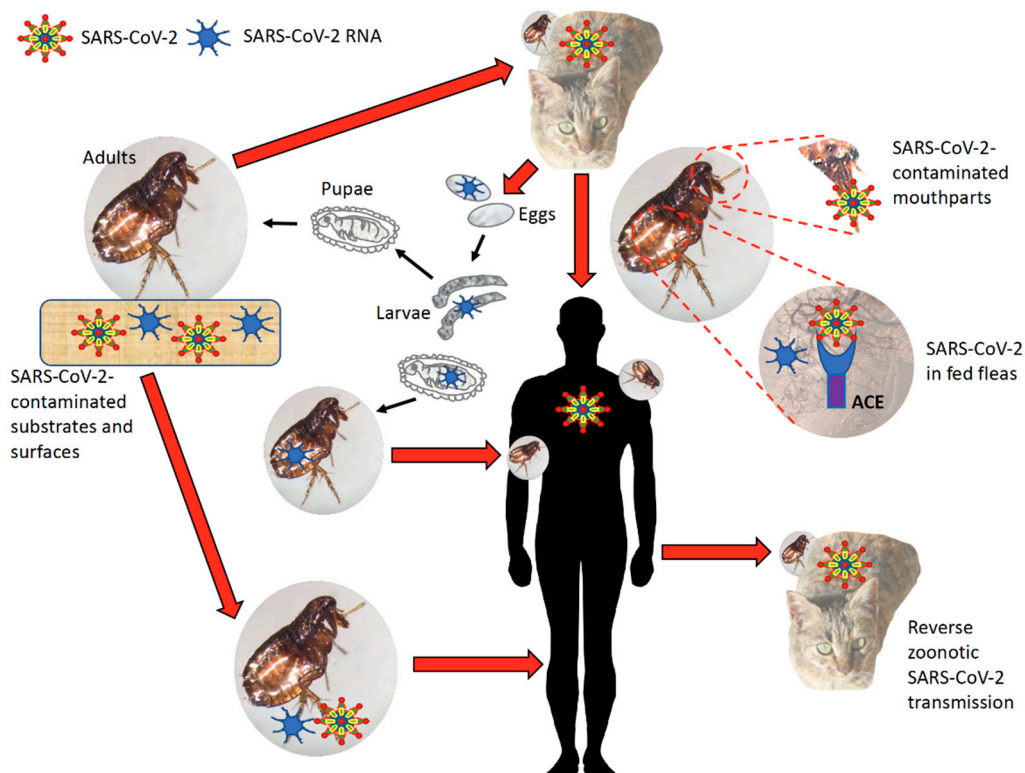


Figure 7. Proposed role of arthropod vectors in SARS-CoV-2 passive transmission. Using flea as a model, coronavirus passive transmission could occur via contact with SARS-CoV-2-contaminated substrates and surfaces. Fleas can feed on SARS-CoV-2-infected animal hosts and virus transmission to humans occurs via contaminated mouthparts, blood-meal regurgitation or inherited virus RNA. Similar to RNAi mechanisms, virus RNA may be also transmitted transovarially and transstadially. Reverse zoonotic SARS-CoV-2 transmission may also occur with arthropod passive vectors.

As with our previous studies of complex stability in mammalian hosts [31], it is important to bear in mind the caveats associated with these types of studies. Although the computational protocol we used (exploiting 3D modelling and mutation studies by mCSM-PPI2) has been validated by experimental results obtained for a number of animal hosts, some of these studies captured in vitro rather than real life data. However, recent reports do support more of our predictions (experimental studies, [6,26,88–92], real-life data, [93–96]) further validating this approach. In addition, despite concerns raised on possible SARS-CoV-2 passive transmission by insects [97–99], recent studies have shown a failure of SARS-CoV-2 to infect or transmit in mosquitos, supporting our calculations on complex stability for this ectoparasite [100,101]. The stabilisation values reported in this manuscript are small, within the range of error for the methods used, suggesting that it is likely that the SARS-CoV-2 S-protein:ACE complex could form in ectoparasites. Although our structural analyses revealed that some key interactions in the interface are lost in the ectoparasite hosts this seems to be compensated by increased numbers of non-covalent interactions between residues in the binding partners. Furthermore, horseshoe bats which have been considered as a putative reservoir host, are reported infected from in vitro experiments, despite considerable disruption in the interface and destabilization of the complex ($\Delta\Delta G$ 3.7). However, whilst supporting the likelihood of complex formation we reiterate that our results do not provide any evidence supporting infection in the ectoparasites. They do prompt some concern though, and suggest that further exploratory experimental studies would be valuable.

Experimental approaches to validate SARS-CoV-2 S-protein:ACE complex formation in ectoparasites and their possible in virus transmission could include (a) evaluation of coronavirus survival in alimentary tract and midgut tissues after contact with SARS-CoV-2 after feeding on infected hosts or exposure to virus-spiked medium [102], (b) artificial injection of SARS-CoV-2 (i.e., intrathoracic inoculation) and sampling at different time points for in vitro titration of virus levels [101], and (c) ability of SARS-CoV-2-exposed ectoparasites to transmit the coronavirus to exposed environments and susceptible experimentally infested animal hosts [102].

Supplementary Materials: The following are available online at <https://www.mdpi.com/article/10.3390/v13040708/s1>, Figure S1: Comparison of LigPlot predicted bonding interactions for B.1.351 clade with human, water flea, body louse and deer tick, Figure S2: Structures of this triple mutant show enhanced H-binding in water flea and body louse, Figure S3: BLAST sequence identities of invertebrate metazoan ACEs and human ACE2, Figure S4: DCEX residue similarities of invertebrate metazoan ACE and human ACE2, Figure S5: Phylogenetic tree of invertebrate metazoan ACE DCEX residues, Figure S6: Predicted $\Delta\Delta G$ values of SARS-CoV-2 Wuhan-Hu-1 S-protein: invertebrate metazoan ACE complexes for direct contact plus extended (DCEX) residues, Figure S7: Predicted $\Delta\Delta G$ values of SARS-CoV-2 N501Y S-protein: invertebrate metazoan ACE complexes for direct contact plus extended (DCEX) residues, Table S1: Normalised DOPE scores of SARS-CoV-2 K417N, E484K, N501Y S-protein: ectoparasite ACE complexes, Table S2: Predicted $\Delta\Delta G$ values of SARS-CoV-2 N501Y S-protein: ectoparasite ACE complexes for direct contact (DC) residues and also for direct contact plus extended (DCEX) residues, Table S3: Invertebrate metazoan ACE sequences studied, Table S4: Mutated DC and DCEX residues and the sum Grantham score of invertebrate metazoan ACEs, Table S5: Normalised DOPE scores of SARS-CoV-2 Wuhan-Hu-1 S-protein: invertebrate metazoan ACE complexes, Table S6: Normalised DOPE scores of SARS-CoV-2 N501Y S-protein: invertebrate metazoan ACE complexes.

Author Contributions: Conceptualization, S.D.L., J.d.I.F. and C.O.; methodology, S.D.L., P.A., S.D.-S., J.d.I.F. and C.O.; software, S.D.L., P.A.; validation, S.D.L., P.A., J.d.I.F. and C.O.; formal analysis, S.D.L., P.A., J.d.I.F. and C.O.; investigation, S.D.L., P.A., S.D.-S., J.d.I.F. and C.O.; resources, S.D.L., P.A., M.V. and C.G.; data curation, S.D.L., P.A.; writing—original draft preparation, S.D.L., P.A., J.d.I.F. and C.O.; writing—review and editing, S.D.L., P.A., J.d.I.F., C.G. and C.O.; visualization, S.D.L., J.d.I.F. and P.A.; supervision, J.d.I.F. and C.O.; project administration, J.d.I.F. and C.O.; funding acquisition, J.d.I.F. and C.O. All authors have read and agreed to the published version of the manuscript.

Funding: S.D.L. is funded by a Fundamental Research Grant Scheme from the Ministry of Higher Education Malaysia [FRGS/1/2020/STG01/UKM/02/3]. P.A. is funded by the Wellcome Trust [Wellcome Trust 221327/Z/20/Z]. S.D.-S. is funded by Junta de Comunidades de Castilla-La Mancha (JCCM), Spain and EU-FEDER (grant GALINFEC SBPLY/17/180501/000185). The APC was funded by the Wellcome Trust.

Institutional Review Board Statement: Not applicable.

Informed Consent Statement: Not applicable.

Data Availability Statement: The authors confirm that the data supporting the findings of this study are available within the article and its supplementary materials.

Acknowledgments: We would like to thank Jonathan Lees for his insightful suggestions.

Conflicts of Interest: The authors declare no conflict of interest. The funders had no role in the design of the study; in the collection, analyses, or interpretation of data; in the writing of the manuscript, or in the decision to publish the results.

References

1. Wall, R. Ectoparasites: Future Challenges in a Changing World. *Vet. Parasitol.* **2007**, *148*, 62–74. [CrossRef]
2. World Health Organization (WHO). Vector Borne Diseases. Available online: <https://www.who.int/news-room/fact-sheets/detail/vector-borne-diseases> (accessed on 1 April 2021).
3. de la Fuente, J.; Estrada-Peña, A. Why New Vaccines for the Control of Ectoparasite Vectors Have Not Been Registered and Commercialized? *Vaccines* **2019**, *7*, 75. [CrossRef]
4. Benelli, G. Pathogens Manipulating Tick Behavior—Through a Glass, Darkly. *Pathogens* **2020**, *9*, 664. [CrossRef] [PubMed]
5. Benelli, G.; Petrelli, R.; Canale, A. Arthropod-Borne Disease Control at a Glance: What’s New on Drug Development? *Molecules* **2020**, *25*, 5175. [CrossRef]
6. Kim, Y.-I.; Kim, S.-G.; Kim, S.-M.; Kim, E.-H.; Park, S.-J.; Yu, K.-M.; Chang, J.-H.; Kim, E.J.; Lee, S.; Casel, M.A.B.; et al. Infection and Rapid Transmission of SARS-CoV-2 in Ferrets. *Cell Host Microbe* **2020**, *27*, 704–709. [CrossRef] [PubMed]
7. de la Fuente, J.; Villar, M.; Cabezas-Cruz, A.; Estrada-Peña, A.; Ayllón, N.; Alberdi, P. Tick–Host–Pathogen Interactions: Conflict and Cooperation. *PLoS Pathog.* **2016**, *12*, e1005488. [CrossRef] [PubMed]
8. Neelakanta, G.; Sultana, H.; Fish, D.; Anderson, J.F.; Fikrig, E. Anaplasma Phagocytophilum Induces Ixodes Scapularis Ticks to Express an Antifreeze Glycoprotein Gene That Enhances Their Survival in the Cold. *J. Clin. Investig.* **2010**, *120*, 3179–3190. [CrossRef] [PubMed]
9. Cabezas-Cruz, A.; Espinosa, P.; Alberdi, P.; de la Fuente, J. Tick–Pathogen Interactions: The Metabolic Perspective. *Trends Parasitol.* **2019**, *35*, 316–328. [CrossRef]
10. Cabezas-Cruz, A.; Estrada-Peña, A.; Rego, R.O.M.; De la Fuente, J. Tick-Pathogen Ensembles: Do Molecular Interactions Lead Ecological Innovation? *Front. Cell. Infect. Microbiol.* **2017**, *7*, 74. [CrossRef]
11. de la Fuente, J.; Lima-Barbero, J.F.; Prado, E.; Pacheco, I.; Alberdi, P.; Villar, M. Anaplasma Pathogen Infection Alters Chemical Composition of the Exoskeleton of Hard Ticks (Acari: Ixodidae). *Comput. Struct. Biotechnol. J.* **2020**, *18*, 253–257. [CrossRef]
12. de la Fuente, J.; Pacheco, I.; Villar, M.; Cabezas-Cruz, A. The Alpha-Gal Syndrome: New Insights into the Tick-Host Conflict and Cooperation. *Parasit. Vectors* **2019**, *12*, 154. [CrossRef]
13. Jones, L.; Davies, C.; Steele, G.; Nuttall, P. A Novel Mode of Arbovirus Transmission Involving a Nonviremic Host. *Science* **1987**, *237*, 775–777. [CrossRef]
14. Randolph, S.E. Ticks Are Not Insects: Consequences of Contrasting Vector Biology for Transmission Potential. *Parasitol. Today* **1998**, *14*, 186–192. [CrossRef]
15. Foil, L.D.; Gorham, J.R. Mechanical Transmission of Disease Agents by Arthropods. In *Medical Entomology*; Eldridge, B.F., Edman, J.D., Eds.; Springer: Dordrecht, The Netherlands, 2000; pp. 461–514. ISBN 978-0-7923-6321-7.
16. Chihota, C.M.; Rennie, L.F.; Kitching, R.P.; Mellor, P.S. Mechanical Transmission of Lumpy Skin Disease Virus by Aedes Aegypti (Diptera: Culicidae). *Epidemiol. Infect.* **2001**, *126*, 317–321. [CrossRef]
17. Tuppurainen, E.S.M.; Lubinga, J.C.; Stoltz, W.H.; Troskie, M.; Carpenter, S.T.; Coetzer, J.A.W.; Venter, E.H.; Oura, C.A.L. Mechanical Transmission of Lumpy Skin Disease Virus by Rhipicephalus Appendiculatus Male Ticks. *Epidemiol. Infect.* **2013**, *141*, 425–430. [CrossRef] [PubMed]
18. Kazimírová, M.; Thangamani, S.; Bartíková, P.; Hermance, M.; Holíková, V.; Štibrániová, I.; Nuttall, P.A. Tick-Borne Viruses and Biological Processes at the Tick-Host-Virus Interface. *Front. Cell. Infect. Microbiol.* **2017**, *7*, 339. [CrossRef] [PubMed]
19. Hornok, S.; Hofmann-Lehmann, R.; de Mera, I.G.F.; Meli, M.L.; Elek, V.; Hajtós, I.; Répási, A.; Gönczi, E.; Tánczos, B.; Farkas, R.; et al. Survey on Blood-Sucking Lice (Phthiraptera: Anoplura) of Ruminants and Pigs with Molecular Detection of Anaplasma and Rickettsia spp. *Vet. Parasitol.* **2010**, *174*, 355–358. [CrossRef] [PubMed]

20. Lubinga, J.C.; Tuppurainen, E.S.M.; Mahlare, R.; Coetzer, J.A.W.; Stoltz, W.H.; Venter, E.H. Evidence of Transstadial and Mechanical Transmission of Lumpy Skin Disease Virus by Amblyomma Hebraeum Ticks. *Transbound. Emerg. Dis.* **2015**, *62*, 174–182. [[CrossRef](#)] [[PubMed](#)]
21. Brown, L.D.; Banajee, K.H.; Foil, L.D.; Macaluso, K.R. Transmission Mechanisms of an Emerging Insect-Borne Rickettsial Pathogen. *Parasit. Vectors* **2016**, *9*, 237. [[CrossRef](#)] [[PubMed](#)]
22. de la Fuente, J.; Van Den Bussche, R.A.; Kocan, K.M. Molecular Phylogeny and Biogeography of North American Isolates of Anaplasma Marginale (Rickettsiaceae: Ehrlichieae). *Vet. Parasitol.* **2001**, *97*, 65–76. [[CrossRef](#)]
23. Scoles, G.A.; Broce, A.B.; Lysyk, T.J.; Palmer, G.H. Relative Efficiency of Biological Transmission of *Anaplasma Marginale* (Rickettsiales: Anaplasmataceae) by *Dermacentor Andersoni* (Acari: Ixodidae) Compared with Mechanical Transmission by *Stomoxys Calcitrans* (Diptera: Muscidae). *J. Med. Entomol.* **2005**, *42*, 668–675. [[CrossRef](#)] [[PubMed](#)]
24. Kocan, K.M.; de la Fuente, J.; Blouin, E.F.; Coetzee, J.F.; Ewing, S.A. The Natural History of Anaplasma Marginale. *Vet. Parasitol.* **2010**, *167*, 95–107. [[CrossRef](#)] [[PubMed](#)]
25. Humphery-Smith, I.; Donker, G.; Turzo, A.; Chastel, C.; Schmidt-Mayerova, H. Evaluation of Mechanical Transmission of HIV by the African Soft Tick, Ornithodoros Moubata. *AIDS* **1993**, *7*, 341–348. [[CrossRef](#)]
26. Shi, J.; Wen, Z.; Zhong, G.; Yang, H.; Wang, C.; Huang, B.; Liu, R.; He, X.; Shuai, L.; Sun, Z.; et al. Susceptibility of Ferrets, Cats, Dogs, and Other Domesticated Animals to SARS–Coronavirus 2. *Science* **2020**, *368*, 1016–1020. [[CrossRef](#)]
27. Zhou, P.; Yang, X.-L.; Wang, X.-G.; Hu, B.; Zhang, L.; Zhang, W.; Si, H.-R.; Zhu, Y.; Li, B.; Huang, C.-L.; et al. A Pneumonia Outbreak Associated with a New Coronavirus of Probable Bat Origin. *Nature* **2020**, *579*, 270–273. [[CrossRef](#)] [[PubMed](#)]
28. Delahay, R.; de la Fuente, J.; Smith, G.; Sharun, K.; Snary, E.; Flores Giron, L.; Nziza, J.; Fooks, A.; Brookes, S.; Lean, F.; et al. Assessing the Risks of SARS-CoV-2 in Wildlife. *One Health Outlook* **2021**, *3*, 7. [[CrossRef](#)]
29. Traavik, T.; Mehl, R. Tick-Borne Viruses in Norway. *Med. Biol.* **1975**, *53*, 621–624.
30. Villar, M.; Fernández de Mera, I.G.; Artigas-Jerónimo, S.; Contreras, M.; Gortázar, C.; de la Fuente, J. Coronavirus in Cat Flea: Findings and Questions Regarding COVID-19. *Parasit. Vectors* **2020**, *13*, 409. [[CrossRef](#)]
31. Lam, S.D.; Bordin, N.; Waman, V.P.; Scholes, H.M.; Ashford, P.; Sen, N.; van Dorp, L.; Rauer, C.; Dawson, N.L.; Pang, C.S.M.; et al. SARS-CoV-2 Spike Protein Predicted to Form Complexes with Host Receptor Protein Orthologues from a Broad Range of Mammals. *Sci. Rep.* **2020**, *10*, 16471. [[CrossRef](#)]
32. Cugini, C.; Medrano, M.; Schwan, T.G.; Coburn, J. Regulation of Expression of the Borrelia Burgdorferi B3-Chain Integrin Ligand, P66, in Ticks and in Culture. *Infect. Immun.* **2003**, *71*, 1001–1007. [[CrossRef](#)]
33. Oliveira, L.G.; Peron, J.P.S. Viral Receptors for Flaviviruses: Not Only Gatekeepers. *J. Leukoc. Biol.* **2019**, *106*, 695–701. [[CrossRef](#)]
34. Mészáros, B.; Sámano-Sánchez, H.; Alvarado-Valverde, J.; Čalyševa, J.; Martínez-Pérez, E.; Alves, R.; Shields, D.C.; Kumar, M.; Rippmann, F.; Chemes, L.B.; et al. Short Linear Motif Candidates in the Cell Entry System Used by SARS-CoV-2 and Their Potential Therapeutic Implications. *Sci. Signal.* **2021**, *14*, eabd0334. [[CrossRef](#)] [[PubMed](#)]
35. Gortázar, C.; del-Río, F.J.R.; Domínguez, L.; de la Fuente, J. Host or Pathogen-Related Factors in COVID-19 Severity? *Lancet* **2020**, *396*, 1396–1397. [[CrossRef](#)]
36. Lan, J.; Ge, J.; Yu, J.; Shan, S.; Zhou, H.; Fan, S.; Zhang, Q.; Shi, X.; Wang, Q.; Zhang, L.; et al. Structure of the SARS-CoV-2 Spike Receptor-Binding Domain Bound to the ACE2 Receptor. *Nature* **2020**, *581*, 1–6. [[CrossRef](#)]
37. Altschul, S.F.; Gish, W.; Miller, W.; Myers, E.W.; Lipman, D.J. Basic Local Alignment Search Tool. *J. Mol. Biol.* **1990**, *215*, 403–410. [[CrossRef](#)]
38. NCBI BLAST, Version 2.6; National Centre for Biotechnology: Bethesda, MD, USA, 2017.
39. Steinegger, M.; Meier, M.; Mirdita, M.; Vöhringer, H.; Haunsberger, S.J.; Söding, J. HH-Suite3 for Fast Remote Homology Detection and Deep Protein Annotation. *BMC Bioinform.* **2019**, *20*, 473. [[CrossRef](#)] [[PubMed](#)]
40. Webb, B.; Sali, A. Comparative Protein Structure Modeling Using MODELLER. *Curr. Protoc. Bioinforma.* **2016**, *54*, 5.6.1–5.6.37. [[CrossRef](#)]
41. MODELLER, Version 9.24; University of California San Francisco: San Francisco, CA, USA, 2020.
42. Shen, M.-Y.; Sali, A. Statistical Potential for Assessment and Prediction of Protein Structures. *Protein Sci. Publ. Protein Soc.* **2006**, *15*, 2507–2524. [[CrossRef](#)]
43. Chan, K.K.; Dorosky, D.; Sharma, P.; Abbasi, S.A.; Dye, J.M.; Kranz, D.M.; Herbert, A.S.; Procko, E. Engineering Human ACE2 to Optimize Binding to the Spike Protein of SARS Coronavirus 2. *Science* **2020**, *369*, 1261–1265. [[CrossRef](#)]
44. Armstrong, D.R.; Berrisford, J.M.; Conroy, M.J.; Gutmanas, A.; Anyango, S.; Choudhary, P.; Clark, A.R.; Dana, J.M.; Deshpande, M.; Dunlop, R.; et al. PDBE: Improved Findability of Macromolecular Structure Data in the PDB. *Nucleic Acids Res.* **2020**, *48*, D335–D343. [[CrossRef](#)]
45. Laskowski, R.A. PDBsum: Summaries and Analyses of PDB Structures. *Nucleic Acids Res.* **2001**, *29*, 221–222. [[CrossRef](#)]
46. Rodrigues, C.H.M.; Myung, Y.; Pires, D.E.V.; Ascher, D.B. MCSM-PPI2: Predicting the Effects of Mutations on Protein–Protein Interactions. *Nucleic Acids Res.* **2019**, *47*, W338–W344. [[CrossRef](#)] [[PubMed](#)]
47. Valdar, W.S.J. Scoring Residue Conservation. *Proteins* **2002**, *48*, 227–241. [[CrossRef](#)]
48. Huang, W.; Lu, S.; Huang, Z.; Liu, X.; Mou, L.; Luo, Y.; Zhao, Y.; Liu, Y.; Chen, Z.; Hou, T.; et al. AlloSite: A Method for Predicting Allosteric Sites. *Bioinformatics* **2013**, *29*, 2357–2359. [[CrossRef](#)] [[PubMed](#)]
49. Li, H.; Chang, Y.-Y.; Lee, J.Y.; Bahar, I.; Yang, L.-W. DynOmics: Dynamics of Structural Proteome and Beyond. *Nucleic Acids Res.* **2017**, *45*, W374–W380. [[CrossRef](#)]

50. Panjkovich, A.; Daura, X. PARS: A Web Server for the Prediction of Protein Allosteric and Regulatory Sites. *Bioinformatics* **2014**, *30*, 1314–1315. [[CrossRef](#)] [[PubMed](#)]
51. Murrell, B.; Wertheim, J.O.; Moola, S.; Weighill, T.; Scheffler, K.; Kosakovsky Pond, S.L. Detecting Individual Sites Subject to Episodic Diversifying Selection. *PLoS Genet.* **2012**, *8*, e1002764. [[CrossRef](#)] [[PubMed](#)]
52. Weaver, S.; Shank, S.D.; Spielman, S.J.; Li, M.; Muse, S.V.; Kosakovsky Pond, S.L. Datamonkey 2.0: A Modern Web Application for Characterizing Selective and Other Evolutionary Processes. *Mol. Biol. Evol.* **2018**, *35*, 773–777. [[CrossRef](#)]
53. Martin, D.P.; Murrell, B.; Golden, M.; Khoosal, A.; Muhire, B. RDP4: Detection and Analysis of Recombination Patterns in Virus Genomes. *Virus Evol.* **2015**, *1*, vev003. [[CrossRef](#)] [[PubMed](#)]
54. Li, Y.; Wang, H.; Tang, X.; Ma, D.; Du, C.; Wang, Y.; Pan, H.; Zou, Q.; Zheng, J.; Xu, L.; et al. SARS-CoV-2 and Three Related Coronaviruses Utilize Multiple ACE2 Orthologs and Are Potently Blocked by an Improved ACE2-Ig. *J. Virol.* **2020**, *94*, e01283-20. [[CrossRef](#)] [[PubMed](#)]
55. Hussain, M.; Jabeen, N.; Amanullah, A.; Baig, A.A.; Aziz, B.; Shabbir, S.; Raza, F. Structural Basis of SARS-CoV-2 Spike Protein Priming by TMPRSS2. *AIMS Microbiol.* **2020**, *6*, 350–360. [[CrossRef](#)]
56. Melin, A.D.; Janiak, M.C.; Marrone, F.; Arora, P.S.; Higham, J.P. Comparative ACE2 Variation and Primate COVID-19 Risk. *Commun. Biol.* **2020**, *3*, 641. [[CrossRef](#)] [[PubMed](#)]
57. Wan, Y.; Shang, J.; Graham, R.; Baric, R.S.; Li, F. Receptor Recognition by the Novel Coronavirus from Wuhan: An Analysis Based on Decade-Long Structural Studies of SARS Coronavirus. *J. Virol.* **2020**, *94*, e00127-20. [[CrossRef](#)] [[PubMed](#)]
58. Grantham, R. Amino Acid Difference Formula to Help Explain Protein Evolution. *Science* **1974**, *185*, 862–864. [[CrossRef](#)]
59. Han, Y.; Král, P. Computational Design of ACE2-Based Peptide Inhibitors of SARS-CoV-2. *ACS Nano* **2020**, *14*, 5143–5147. [[CrossRef](#)] [[PubMed](#)]
60. Pettersen, E.F.; Goddard, T.D.; Huang, C.C.; Couch, G.S.; Greenblatt, D.M.; Meng, E.C.; Ferrin, T.E. UCSF Chimera—a Visualization System for Exploratory Research and Analysis. *J. Comput. Chem.* **2004**, *25*, 1605–1612. [[CrossRef](#)] [[PubMed](#)]
61. UCSF Chimera, Version 1.15; University of California San Francisco: San Francisco, CA, USA, 2020.
62. Nakamura, T.; Yamada, K.D.; Tomii, K.; Katoh, K. Parallelization of MAFFT for Large-Scale Multiple Sequence Alignments. *Bioinforma. Oxf. Engl.* **2018**, *34*, 2490–2492. [[CrossRef](#)]
63. Geneious Prime, Version 2.2; Biomatters, Ltd.: Auckland, New Zealand, 2006.
64. Darriba, D.; Taboada, G.L.; Doallo, R.; Posada, D. JModelTest 2: More Models, New Heuristics and Parallel Computing. *Nat. Methods* **2012**, *9*, 772. [[CrossRef](#)] [[PubMed](#)]
65. Miura, R.M. *Some Mathematical Questions in Biology: DNA Sequence Analysis*; American Mathematical Soc: New York, USA, 1986; ISBN 978-0-8218-9711-9.
66. Kumar, S.; Stecher, G.; Li, M.; Knyaz, C.; Tamura, K. MEGA X: Molecular Evolutionary Genetics Analysis across Computing Platforms. *Mol. Biol. Evol.* **2018**, *35*, 1547–1549. [[CrossRef](#)]
67. MEGAX, Version January 2021; Pennsylvania State University: Pennsylvania, PA, USA, 2021.
68. Howe, K.L.; Contreras-Moreira, B.; De Silva, N.; Maslen, G.; Akanni, W.; Allen, J.; Alvarez-Jarreta, J.; Barba, M.; Bolser, D.M.; Cambell, L.; et al. Ensembl Genomes 2020—Enabling Non-Vertebrate Genomic Research. *Nucleic Acids Res.* **2020**, *48*, D689–D695. [[CrossRef](#)]
69. Madeira, F.; Park, Y.M.; Lee, J.; Buso, N.; Gur, T.; Madhusoodanan, N.; Basutkar, P.; Tivey, A.R.; Potter, S.C.; Finn, R.D.; et al. The EMBL-EBI Search and Sequence Analysis Tools APIs in 2019. *Nucleic Acids Res.* **2019**, *47*, W636–W641. [[CrossRef](#)] [[PubMed](#)]
70. Lam, S.D.; Das, S.; Sillitoe, I.; Orengo, C. An Overview of Comparative Modelling and Resources Dedicated to Large-Scale Modelling of Genome Sequences. *Acta Crystallogr. Sect. Struct. Biol.* **2017**, *73*, 628–640. [[CrossRef](#)]
71. Lam, S.D.; Dawson, N.L.; Das, S.; Sillitoe, I.; Ashford, P.; Lee, D.; Lehtinen, S.; Orengo, C.A.; Lees, J.G. Gene3D: Expanding the Utility of Domain Assignments. *Nucleic Acids Res.* **2016**, *44*, D404–D409. [[CrossRef](#)] [[PubMed](#)]
72. Laskowski, R.A.; Swindells, M.B. LigPlot+: Multiple Ligand-Protein Interaction Diagrams for Drug Discovery. *J. Chem. Inf. Model.* **2011**, *51*, 2778–2786. [[CrossRef](#)]
73. Shang, J.; Ye, G.; Shi, K.; Wan, Y.; Luo, C.; Aihara, H.; Geng, Q.; Auerbach, A.; Li, F. Structural Basis of Receptor Recognition by SARS-CoV-2. *Nature* **2020**, *581*, 221–224. [[CrossRef](#)]
74. Brielle, E.S.; Schneidman-Duhovny, D.; Linial, M. The SARS-CoV-2 Exerts a Distinctive Strategy for Interacting with the ACE2 Human Receptor. *Viruses* **2020**, *12*, 497. [[CrossRef](#)]
75. Wrapp, D.; Wang, N.; Corbett, K.S.; Goldsmith, J.A.; Hsieh, C.-L.; Abiona, O.; Graham, B.S.; McLellan, J.S. Cryo-EM Structure of the 2019-nCoV Spike in the Prefusion Conformation. *Science* **2020**, *367*, 1260–1263. [[CrossRef](#)] [[PubMed](#)]
76. Gray, S.M.; Banerjee, N. Mechanisms of Arthropod Transmission of Plant and Animal Viruses. *Microbiol. Mol. Biol. Rev.* **1999**, *63*, 128–148. [[CrossRef](#)]
77. Goldman, E. Exaggerated Risk of Transmission of COVID-19 by Fomites. *Lancet Infect. Dis.* **2020**, *20*, 892–893. [[CrossRef](#)]
78. Fernández-de-Mera, I.G.; Rodríguez del-Río, F.J.; Fuente, J.; Pérez-Sancho, M.; Hervás, D.; Moreno, I.; Domínguez, M.; Domínguez, L.; Gortázar, C. Detection of Environmental SARS-CoV-2 RNA in a High Prevalence Setting in Spain. *Transbound. Emerg. Dis.* **2020**, tbed.13817. [[CrossRef](#)]
79. de la Fuente, J.; Kocan, K.M.; Almazán, C.; Blouin, E.F. RNA Interference for the Study and Genetic Manipulation of Ticks. *Trends Parasitol.* **2007**, *23*, 427–433. [[CrossRef](#)]

80. de la Fuente, J.; Estrada-Peña, A.; Cabezas-Cruz, A.; Brey, R. Flying Ticks: Anciently Evolved Associations That Constitute a Risk of Infectious Disease Spread. *Parasit. Vectors* **2015**, *8*, 538. [[CrossRef](#)]
81. Oguntomole, O.; Nwaeze, U.; Eremeeva, M. Tick-, Flea-, and Louse-Borne Diseases of Public Health and Veterinary Significance in Nigeria. *Trop. Med. Infect. Dis.* **2018**, *3*, 3. [[CrossRef](#)]
82. Linardi, P.M.; de Avelar, D.M. Neosomes of Tungid Fleas on Wild and Domestic Animals. *Parasitol. Res.* **2014**, *113*, 3517–3533. [[CrossRef](#)]
83. Barker, S.C. Phylogeny and Classification, Origins, and Evolution of Host Associations of Lice. *Int. J. Parasitol.* **1994**, *24*, 1285–1291. [[CrossRef](#)]
84. Contreras, M.; Villar, M.; Artigas-Jerónimo, S.; Kornieieva, L.; Mytrofanov, S.; de la Fuente, J. A Reverse Vaccinology Approach to the Identification and Characterization of Ctenocephalides Felis Candidate Protective Antigens for the Control of Cat Flea Infestations. *Parasit. Vectors* **2018**, *11*, 43. [[CrossRef](#)]
85. Villar, M.; Pacheco, I.; Merino, O.; Contreras, M.; Mateos-Hernández, L.; Prado, E.; Barros-Picanço, D.K.; Lima-Barbero, J.F.; Artigas-Jerónimo, S.; Alberdi, P.; et al. Tick and Host Derived Compounds Detected in the Cement Complex Substance. *Biomolecules* **2020**, *10*, 555. [[CrossRef](#)] [[PubMed](#)]
86. Zhu, K.Y.; Palli, S.R. Mechanisms, Applications, and Challenges of Insect RNA Interference. *Annu. Rev. Entomol.* **2020**, *65*, 293–311. [[CrossRef](#)] [[PubMed](#)]
87. McElroy, K.M.; Blagburn, B.L.; Breitschwerdt, E.B.; Mead, P.S.; McQuiston, J.H. Flea-Associated Zoonotic Diseases of Cats in the USA: Bartonellosis, Flea-Borne Rickettsioses, and Plague. *Trends Parasitol.* **2010**, *26*, 197–204. [[CrossRef](#)]
88. Lu, S.; Zhao, Y.; Yu, W.; Yang, Y.; Gao, J.; Wang, J.; Kuang, D.; Yang, M.; Yang, J.; Ma, C.; et al. Comparison of nonhuman primates identified the suitable model for COVID-19. *Signal Transduct. Target. Ther.* **2020**, *5*, 157. [[CrossRef](#)] [[PubMed](#)]
89. Shan, C.; Yao, Y.-F.; Yang, X.-L.; Zhou, Y.-W.; Wu, J.; Gao, G.; Peng, Y.; Yang, L.; Hu, X.; Xiong, J.; et al. Infection with Novel Coronavirus (SARS-CoV-2) Causes Pneumonia in the Rhesus Macaques. *Cell Res.* **2020**, *30*, 670–677. [[CrossRef](#)] [[PubMed](#)]
90. Liu, Y.; Hu, G.; Wang, Y.; Ren, W.; Zhao, X.; Ji, F.; Zhu, Y.; Feng, F.; Gong, M.; Ju, X.; et al. Functional and Genetic Analysis of Viral Receptor ACE2 Orthologs Reveals a Broad Potential Host Range of SARS-CoV-2. *Proc. Natl. Acad. Sci. USA* **2021**, *118*, e2025373118. [[CrossRef](#)] [[PubMed](#)]
91. Zhao, X.; Chen, D.; Szabla, R.; Zheng, M.; Li, G.; Du, P.; Zheng, S.; Li, X.; Song, C.; Li, R.; et al. Broad and Differential Animal ACE2 Receptor Usage by SARS-CoV-2. *J. Virol.* **2020**, *94*, e00940-20. [[CrossRef](#)]
92. Liu, Z.; Xiao, X.; Wei, X.; Li, J.; Yang, J.; Tan, H.; Zhu, J.; Zhang, Q.; Wu, J.; Liu, L. Composition and Divergence of Coronavirus Spike Proteins and Host ACE2 Receptors Predict Potential Intermediate Hosts of SARS-CoV-2. *J. Med. Virol.* **2020**, *92*, 595–601. [[CrossRef](#)] [[PubMed](#)]
93. Elbe, S.; Buckland-Merrett, G. Data, Disease and Diplomacy: GISAID's Innovative Contribution to Global Health: Data, Disease and Diplomacy. *Glob. Chall.* **2017**, *1*, 33–46. [[CrossRef](#)] [[PubMed](#)]
94. McAloose, D.; Laverack, M.; Wang, L.; Killian, M.L.; Caserta, L.C.; Yuan, F.; Mitchell, P.K.; Queen, K.; Mauldin, M.R.; Cronk, B.D.; et al. From People to Panthera: Natural SARS-CoV-2 Infection in Tigers and Lions at the Bronx Zoo. *Microbiology* **2020**, *11*, e02220-20.
95. Shu, Y.; McCauley, J. GISAID: Global Initiative on Sharing All Influenza Data—from Vision to Reality. *Eur. Surveill. Bull. Eur. Sur Mal. Transm. Eur. Commun. Dis. Bull.* **2017**, *22*, 30494. [[CrossRef](#)]
96. Zhang, Q.; Zhang, H.; Huang, K.; Yang, Y.; Hui, X.; Gao, J.; He, X.; Li, C.; Gong, W.; Zhang, Y.; et al. SARS-CoV-2 Neutralizing Serum Antibodies in Cats: A Serological Investigation. *Microbiol. Emerg. Microbes Infect.* **2020**, *9*, 2013–2019. [[CrossRef](#)]
97. Ismail, M.; Verma, A.; Abdulkadir, A.; Kumar, A.; Dhawan, D.; Bolya, K.; Barik, M. Possible Mechanical Transmission of SARS-CoV-2 Causing COVID-19 by Insects: Infection, Prevention, Implications, and Control. *Open J. Med. Microbiol.* **2020**, *10*, 89–101. [[CrossRef](#)]
98. Dehghani, R.; Kassiri, H. A Brief Review on the Possible Role of Houseflies and Cockroaches in the Mechanical Transmission of Coronavirus Disease 2019 (COVID-19). *Arch. Clin. Infect. Dis* **2020**, *15*, e102863. [[CrossRef](#)]
99. Montes, A.; Coronell, W.; Baldiris, R. Can house flies mechanically carry and/or transport sars-cov-2? *Int J. Clin. Virol.* **2020**, *4*, 76–78. [[CrossRef](#)]
100. Fortuna, C.; Montarsi, F.; Severini, F.; Marsili, G.; Toma, L.; Amendola, A.; Bertola, M.; Michelutti, A.; Ravagnan, S.; Capelli, G.; et al. The Common European Mosquitoes Culex Pipiens and Aedes Albopictus Are Unable to Transmit SARS-CoV-2 after a Natural-Mimicking Challenge with Infected Blood. *Parasit. Vectors* **2021**, *14*, 76. [[CrossRef](#)] [[PubMed](#)]
101. Huang, Y.-J.S.; Vanlandingham, D.L.; Bilyeu, A.N.; Sharp, H.M.; Hettenbach, S.M.; Higgs, S. SARS-CoV-2 Failure to Infect or Replicate in Mosquitoes: An Extreme Challenge. *Sci. Rep.* **2020**, *10*, 11915. [[CrossRef](#)] [[PubMed](#)]
102. Calibeo-Hayes, D.; Denning, S.S.; Stringham, S.M.; Guy, J.S.; Smith, L.G.; Watson, D.W. Mechanical transmission of turkey coronavirus by domestic houseflies (*Musca domestica* Linnaeus). *Avian Dis.* **2003**, *47*, 149–153. [[CrossRef](#)]